Personal Account

DOI: 10.1002/tcr.201800153

THE CHEMICAL RECORD

Progress on the Photocatalytic Reduction Removal of Chromium Contamination

Zengying Zhao,[a] He An,[a] Jing Lin,*[b] Mingchao Feng,[a] Vignesh Murugadoss,[c, d, e] Tao Ding,*[e] Hu Liu,[c, f] Qian Shao,[g] Xianmin Mai,*[h] Ning Wang,[i] Hongbo Gu,[j] Subramania Angaiah,*[d] and Zhanhu Guo*[c]

Abstract: Rapid industrialization leads to increased wastewater discharge encompassing hexavalent chromium (Cr(VI)), which leads to serious environmental problems of toxicity and potential carcinogenicity. Removal of these species is normally carried out by ion-exchange, precipitation, membrane filtration, sorption, photocatalytic reduction, etc. This review mainly focuses on the photocatalytic and photoelectrocatalytic (PEC) reduction of Cr (VI), because of their advantages over other methods such as reduced risk of secondary pollution by non-reduced Cr (VI), no sludge formation, no need for a large amount of chemical reagents, clean and easy installation. The main factors influencing the photocatalytic reduction efficiency of Cr (VI) such as catalyst activity, solution pH, Cr adsorption on the catalyst and additives, are briefly discussed. Finally, a special emphasis is provided to the photoelectrocatalytic (PEC) reduction of Cr (VI).

Keywords: Chromium removal, Photocatalytic reduction, Photoelectrocatalytic reduction

1. Chromium Pollution

Chromium (Cr) is one of the most important industrial raw materials, used in leather tanning, electroplating, metal finishing, magnetic tapes, pigments, electrical or electronic equipment, and catalysis, etc.[1] Chromium contamination in surface and groundwater is becoming a serious concern due to emissions from industrial processes. Due to the danger to the environment and the accumulation in the food chain, the removal of Cr attracts increasing attention.[2] For example, it is one of the sixteen most toxic pollutants because of its

[a] *Z. Zhao, H. An, M. Feng*
School of Science, China University of Geosciences, Beijing 100083, China
[b] *J. Lin*
School of Chemistry and Chemical Engineering, Guangzhou University, Guangzhou 510006, China
E-mail: linjing@gzhu.edu.cn
[c] *V. Murugadoss, H. Liu, Z. Guo*
Chemical and Biomolecular Engineering Department, University of Tennessee, Knoxville, TN 37996, USA
E-mail: zguo10@utk.edu
[d] *V. Murugadoss, S. Angaiah*
Electrochemical Energy Research Lab, Centre for Nanoscience and Technology, Pondicherry University, Puducherry-605 014, India
E-mail: a.subramania@gmail.com
[e] *V. Murugadoss, T. Ding*
College of Chemistry and Chemical Engineering, Henan University, Kaifeng 475004, China
E-mail: dingtao@henu.edu.cn
[f] *H. Liu*
Key Laboratory of Materials Processing and Mold (Zhengzhou University), Ministry of Education; National Engineering Research Center for Advanced Polymer Processing Technology, Zhengzhou University, Zhengzhou, 450002, China
[g] *Q. Shao*
College of Chemical and Environmental Engineering, Shandong University of Science and Technology, Qingdao, Shandong, 266590, China
[h] *X. Mai*
School of Urban Planning and Architecture, Southwest Minzu University, Chengdu 610041, China
E-mail: myzjx0329@163.com
[i] *N. Wang*
State Key Laboratory of Marine Resource Utilization in South China Sea, Hainan University, Haikou 570228, China
[j] *H. Gu*
Shanghai Key Lab of Chemical Assessment and Sustainability, Department of Chemistry, Tongji University, Shanghai 200092, China

teratogenic and carcinogenic effect on human health,[3] and has also been recognized by the United State Environmental Protection Agency (USEPA) as Group A carcinogen.[4] Therefore, the USEPA and the World Health Organization (WHO) have set the maximum contaminant levels (MCL) in drinking water at 0.1 mg/L and 0.05 mg/L for chromium.[5]

Chromium presents as bichromate ($HCrO_4^-$) or chromate (CrO_4^{2-}) in water system depending on their pH and the Cr(VI) is negatively charged in all forms. At pH <6.8, the $HCrO_4^-$ and H_2CrO_4 are predominantly present, while at pH >6.8, CrO_4^{2-} alone is stable.[6] The oxy-anions in the CrO_4^{2-} are reduced to their trivalent form Cr(III) by accepting electrons from the reducing reagents present in the solution. The rate of Cr(VI) reduction increases with the decrease in pH of the solution. The reduced Cr(III) is less toxic than the Cr(VI). Hence, the reduction of Cr(VI) to Cr(III) is not a thorough solution as its toxicity poses a threat to the environment and human health. Since Cr(III) is comparatively more stable with respect to the oxidation-reduction potential, it cannot be easily reduced.[7] Therefore, the reduction of Cr(VI) to Cr(III) and simultaneous adsorption of the reduced Cr (III) could be the feasible solution for effective chromium removal.[8] At pH 8 or higher, Cr(III) can react easily with particulates to form insoluble metal salts such as $Cr(OH)_3$ in water.[9]

2. Chromium Pollution Treatment Methods

Although Cr exists in several valence states (from -2 to $+6$), the less toxic Cr^{3+} and more toxic Cr^{6+} are the major pollutants found in the environment.[10] As for the removal of Cr(VI), the methods have involved in the use of cationic and anionic ion-exchange resins,[11] chemical precipitation,[12] membrane filtration,[13] sorption,[14] biological method,[15] and photocatalytic reduction.[16]

However, no perfect methods can overcome the problems completely from the pollution treatment cost, process complexity, damage to the environment and removal efficiency. Thereinto, the photocatalytic reduction method is a kind of green, low-cost method. But the efficiency needs to be urgently improved.

3. Some New Adsorbent Materials for Cr Pollution

Adsorption methods are preferred to various conventional methods for Cr (VI) removal due to less expensive. In recent years, research interest focuses on low-cost adsorbents such as activated carbon.[16a,17] Especially, because of the low cost and local availability, natural materials such as chitosan,[18] gum,[15b] fungal mycelia,[15c] sulfate-reducing bacteria,[19] or certain waste products from industrial operations are modified for the adsorption of Cr(VI).[14a,c] Some examples are as follows:

3.1. Organomodified Diatomaceous Earth

Diatomaceous earth (DAT) has been used in the removal of Cr(VI).[20] The adsorption capacity of DAT was improved using a cationic surfactant, hexadecyltrimethylammonium bromide (HDTMABr), by ion exchange reaction. The Cr(III) and Cr(VI) ions were adsorbed onto natural DAT and organomodified DAT-HDTMABR from aqueous solutions. The adsorption process is relatively faster and the equilibrium is established quicker for DAT-HDTMABR than for DAT. The results show that organomodified diatomaceous earth has more metal ion removal (%R) and adsorption capacity than the natural material. Therefore, the authors concluded that the ion-exchange mechanism of the modified method is feasible.[4b,21]

3.2. Nano-γ-Al_2O_3 by the Novel Sol-Gel Method

Al_2O_3 has been adopted in Cr(VI) removal for several cases.[22] Recently, Shokati et al. prepared a novel nano-γ-Al_2O_3 adsorbent using the sol-gel method. The adsorption isotherms for Cr(VI) well fitted with the Langmuir adsorption isotherm equations. The adsorbent has a good capacity to adsorb Cr(VI) with a maximum capacity of 13.3 mg/g. The sorption capacity doesn't change remarkably after reusing the sorbent for sorption-desorption cycle, so the synthesized nano-γ-Al_2O_3 can be reusable with high efficiency and can be used in water and wastewater treatment for Cr(VI) removal.[14a]

3.3. Modified Magnetic Iron Oxide

Although the synthesis of magnetite nanoparticles is tedious, it is still the best adsorbent for Cr(VI) from wastewater.[23] This is attributed to their high gradient magnetic field that improves the separation of the liquid-solid mixture.[24] Sponge-like carbon matrix consists of zerovalent iron nanoparticles following the pseudo-second order and Langmuir isotherm towards Cr(VI) removal. It was observed that the chromium removal capacity increased with increasing the annealing temperature from 500 to 800 °C at the optimum pH of 3.0. This is attributed to the improved amorphous nature of the carbon with more disordered bonds and magnetic property of zerovalent iron nanoparticles at a higher annealing temperature.[13b,25] The new tendency in this field is the magnetic nanoparticles (MNPs) composited with a surfactant or environment-friendly natural polymers, such as a polysaccharide, etc. The hydrogel nanocomposites comprised of Gum karaya-grafted poly (acrylamide-co-acrylic

acid) and an iron oxide magnetic exhibited great potential towards Cr(VI) ions removal as an adsorbent, to improve the quality of mine effluents prior to discharge in the environment.[15b]

3.4. PAN-$FeCl_2$ Composite Adsorbent

Nanoparticle adsorbents are easier to be prepared compared with the above adsorbents, but the small particle size often leads to material wastage and recoverability problems.[26] While nanofibers can be used as the adsorbents for various applications without the above-mentioned problems. Polyacrylonitrile (PAN) nanofiber can be composited with $Mn(CH_3COO)_2$,[27] TiO_2[28] etc. to remove Cr(VI), because its CN group can interact with the metal ions to improve the adsorption abilities.[29] Electrospun nanofibrous PAN/$FeCl_2$ composites exhibited excellent performance in Cr removal, with the maximum adsorption of chromium ions of 108 mg Cr/g $FeCl_2$.[30]

3.5. Chitosan Derivatives

Chitosan is a biopolymer derived from chitin, a most abundant source of the biopolymer, by deacetylation.[31] Chitosan has been mainly used as its derivatives in the Cr(VI) ion removal, as the primary amine group at the C-2 position of its pyranoside ring eases the preparation of different derivatives having excellent chemical properties.[32] Besides, it also can be used in the same field when composited with other materials.[33] A chitosan derivate obtained by quaternization of the amine group of chitosan and esterification of hydroxyl groups with Ethylenediaminetetraacetic acid (EDTA) dianhydride, exhibited zwitterionic characteristics. The maximum adsorption capacity of the chitosan derivate is 1.910 mmol/g, and it can still adsorb both metallic cations and oxyanions of Cr(VI) with certain efficiency when it is recovered by 0.1 mol/L HNO_3 and subjected to re-adsorption.[18a]

3.6. PANI Composites

The PANI can act as the reducing agent for reduction of Cr(VI) to Cr(III) as well as the adsorbent for the Cr(III), and hence attracted attention towards the removal of Cr(VI) contaminants.[6,34] For examples, the coating of PANI on magnetic Fe_3O_4, cellulose, and carbon fabric are reported as adsorbents as well as reductants for the Cr(VI) removal.[6,34a] In all the cases, the incorporation of PANI enhances both the removal capacity and rate of Cr(VI) removal. This is attributed to the improved hydrophilicity of the composites by the introduction of PANI. The mechanism of chromium removal of the PANI-based composites is briefed below; Firstly, the Cr(VI) adsorbed on the surface of the PANI based composites is reduced to Cr(III) by their amine groups. Later, the composites can be regenerated by removing the electrostatically adsorbed Cr(III) by the acid treatments.

4. Photocatalytic Reduction for the Cr(VI) Removal

4.1. Photocatalytic Reduction

Photo-catalytic reduction of Cr(VI) ions to Cr(III) ions is more practical and cleaner compared to chemical reduction.[35] The widely reported photo-catalytic reductants are metal oxides and metal sulfides, including ZnO,[35a] TiO_2,[36] WO_3,[37] MnS,[38] CdS,[39] In_2O_3,[40] etc. The heterogeneous photocatalysis (HP), as a relatively new technique for water or air purification can work under natural sunlight. Therefore, it is an appealing opportunity for green chemistry. Some important factors influencing photoreduction efficiency are as follows:

4.1.1. Catalyst's Ability

When the semiconductor photocatalyst is illuminated by light having an energy greater than its band gap energy, electron-hole pairs are generated and transferred to their conduction band (CB) and valence band (VB), respectively.[36] Cr(VI) is reduced by the photo-excited CB electrons, at the same time water is oxidized by the photo-excited VB holes. To achieve the photoreduction of Cr(VI), the CB of the semiconductors (for example, CB is −0.42 for TiO_2) must be more negative comparing to the reduction potential of Cr(VI) (i.e. ~0.36 at pH 7 as shown in Figure 1).

Thus the energy level of CB indicates the potential of a semiconductor towards Cr(VI) reduction. Also, the position of CB and VB is influenced by the pH. The increase in pH of the electrolyte solution shifts the VB and CB towards more cathodic potentials by 59 mV per pH unit as shown in Equation (1) and (2).[41]

$$E_{CB}(V) = -0.05 - 0.059\,pH \text{ (at } 25\,^{\circ}C) \quad (1)$$

$$E_{VB}(V) = 3.15 - 0.059\,pH \text{ (at } 25\,^{\circ}C) \quad (2)$$

Also, the reduction potential of Cr(VI) becomes more negative at higher pH compared to the photogenerated electrons. Consequently, the photocatalytic reduction of the Cr(VI) ion is favored at a lower pH. Although the driving force of the Cr(VI) reduction decreases with increasing their concentration, it can be reduced photocatalytically to down to 10^{-12} M, thermodynamically.[36] Since the reduction

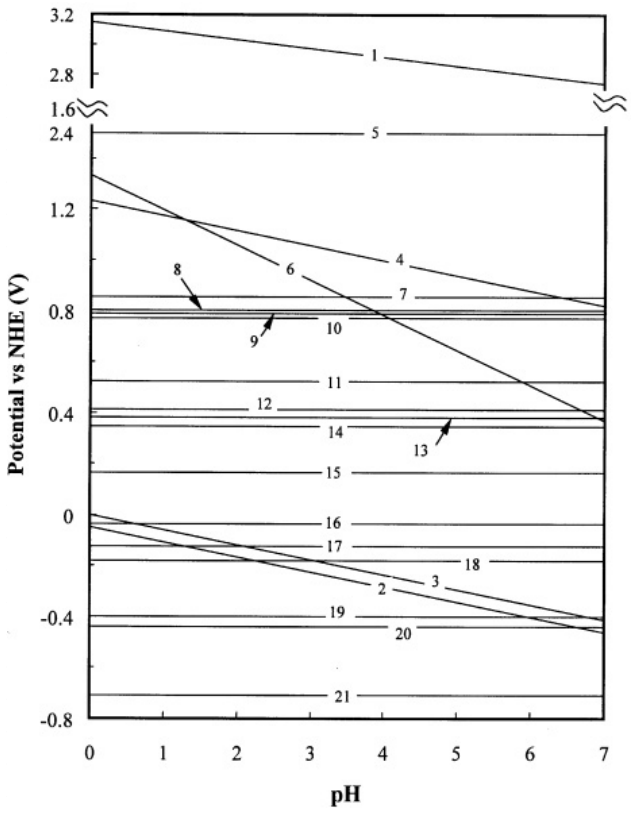

Figure 1. Pourbaix diagram showing positions of valence and condition bands of anatase TiO_2 along with the reduction potentials of metal ions (1 M) at different pH (calculated from the Nernst equation) 1 E_{VB}; 2E_{CB}; $3\varphi_{H^+/H_2}$; $4\varphi_{O_2/H_2O}$; $5\varphi_{Au^{2+}/Au}$; $6\varphi_{Cr^{6+}/Cr^{3+}}$; $7\varphi_{Hg^{2+}/Hg}$; $8\varphi_{Ag^{2+}/Ag}$; $9\varphi_{Hg_2^{2+}/Hg}$; $10\varphi_{Fe^{3+}/Fe^{2+}}$; $11\varphi_{Cu^{+}/Cu}$; $12\varphi_{HgCl_2/Hg}$; $13\varphi_{HgCl_4^{2-}/Hg}$; $14\varphi_{Cu^{2+}/Cu}$; $15\varphi_{Cu^{2+}/Cu^{+}}$; $16\varphi_{Fe^{3+}/Fe}$; $17\varphi_{Pb^{2+}/Pb}$; $18\varphi_{Ni^{2+}/Ni}$; $19\varphi_{Cd^{2+}/Cd}$; $20\varphi_{Fe^{2+}/Fe}$; $21\varphi_{Cr^{3+}/Cr}$. Reproduced with permission from ref. [36] Copyrights © 2001 Elsevier Science Ltd.

potential of Cr(III) is more negative than that of Cr (VI), it cannot be reduced photocatalytically.

4.1.2. Solution pH and Cr Adsorption on the Catalyst

Similar to the pH, the adsorption of Cr(VI) onto the catalyst surface is another important parameter that influences the photocatalytic reduction. At pH values less than 2.0, Cr(VI) exists as H_2CrO_4. The surface of the catalyst (TiO_2, for example) with the positive charges leads to a weaker Cr(VI) adsorption, so the degradation rate of Cr(VI) is relatively lower. By increasing the pH from 2.0 to 4.0, the concentration of anions (that is $HCrO_4^-$ and CrO_4^{2-}) gets increased, improving the adsorption on the catalyst surface, and thus increases their degradation rate. The TiO_2 surface has greater positive charges at pH less than 3.0 that neutralizes the photogenerated electrons, and thus their photocatalytic efficiency gets decreased. However, at pH greater than 4.0, the surface charge of TiO_2 decreases, thereby reducing the adsorption of chromium ions and subsequently slowing down the photocatalytic reaction.[42]

4.1.3. Effects of Additives

Usually, many studies reported only the photocatalytic reduction activity of catalyst with Cr(VI), and there are only a few reports regarding the decontamination of organic species at the same time. However, the coexistence of Cr(VI) and organic species is the actual situations in the real environmental pollution.[43]

The above-mentioned organic species include both the aromatic compounds and non-aromatic compounds. The former tends to form quinone and polyhydroxy derivatives at the first stage of photodegradation, which in turn results in the formation of metal complexes on the catalyst's surface and deactivate it. While the non-aromatic compounds tend to form a double bond by a dehydration process that then leads to the cracking of that molecule into a shorter one. Therefore, the nonaromatic compounds do not generate the metal complexes which are not supposed to be "harmful" for photocatalyst activity.[44]

Fortunately, it has been reported that the addition of certain organic acids improves the rate of Cr(VI) photocatalytic reduction. For example, the addition of citric acid promotes the electron capturing ability of Cr(VI) as it acts as a hole scavenger and thereby increases the photocatalytic reduction rate of Cr(VI).[45] Also, citric acid has no negative effect on the catalyst activity.[44] Besides, as a sacrificial agent, the carboxylic acid plays a key role in the photoreduction of Cr(VI) by suppressing the recombination of the photogenerated electron-hole pairs.[45] For example, H. Fu et al. reported that the presence of 4-chlorophenol along with Cr(VI) enhanced the photocatalytic efficiency by the synergic redox reaction.[46] This reduced the electron-hole recombination as both the oxidation reaction and reduction reaction took place simultaneously. The synergic redox reaction refers to the following two half redox semi-reactions that occur simultaneously. One is the decontamination of the metal ions (chromium ions) by accepting the photo-generated electrons and the other is the decontamination of organic species by accepting the photo-generated holes (4-chlorophenol). Rubina et al. reported that the addition of citric acid enhanced the reduction rate of $TiO_2/H_2O_2/UV$, demonstrating the hole scavenging nature of citric acid. Also, it was observed that citric acid in combination with H_2O_2 exhibited a higher TiO_2 photocatalytic reduction rate than the system without H_2O_2.[47] The dissolved oxygen can also improve the

reduction rate of Cr(VI). However, there is also literature from a different viewpoint.[44] The discrepancies are proposed to be due to varying solution conditions under which the experiments were performed by different researchers.

4.2. Recent Research of Photocatalyst for Cr(VI) Reduction

4.2.1. TiO_2 and Titanate Nanotube

TiO_2 is the most widely investigated photocatalyst, exhibiting good photocatalytic performance and stability in aqueous media under illumination.[36,48] For example, Cr(VI) can be easily reduced with TiO_2 as catalyst under UV irradiation, which obeys the Langmuir-Hinshelwood (L–H) kinetic equation. For example, D. Chen et al. investigated physical adsorption and photocatalytic reduction of Cr(VI) in the suspensions of Degussa P25. The results reveal that Degussa P25 exhibited good photocatalytic activity towards Cr(VI) reduction (Figure 2). However, the dissolved oxygen inhibited the photocatalytic reduction of Cr(VI) significantly by acting as an electron acceptor. This problem was overcome by using organic reductants, such as Ethylenediaminetetraacetic acid (EDTA). The organic reductants facilitated the direct electron transfer to the VB and thereby promoted their photocatalytic reduction ability.[41]

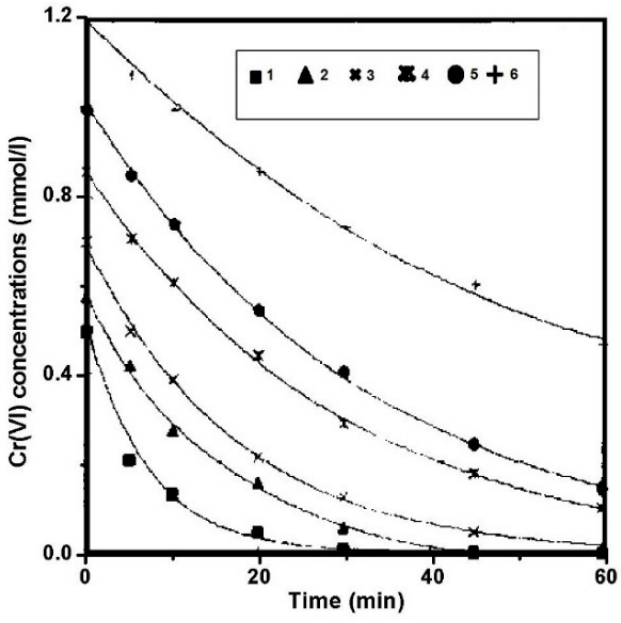

Figure 2. Cr(VI) ion concentrations on TiO_2 with different Cr(VI) initial concentrations under UV irradiation. Reaction condition: TiO_2 concentration: 1 g/l; pH 2.5; light source; 250-W mercury lamp; room temperature; air atmosphere; Cr(VI) initial concentrations (mmol/l): (1) 0.48; (2) 0.57; (3) 0.70; (4) 0.86; (5) 1.00; (6) 1.23. Reproduced with permission from ref.[46] Copyrights © 1998 Elsevier Science S.A.

In addition to the two-step conventional method involving the Cr(VI) photocatalytic reduction and then Cr(III) adsorption, one-step method has also been reported by using the mixture of TiO_2 and titanate nanotubes (TNT). The proposed single-step process reduced the reaction time for over 50% and thereby doubled the chromium removal rate.[8]

However, the "general concept" that "TiO_2 would be an effective photocatalyst for the treatment of Cr(VI) in acidic media" becomes unsettled. For example, Khalil et al. investigated the photoreduction capability of different semiconductors such as ZnO, Hombikat UV100, Degussa P25, and WO_3. They concluded that the photocatalytic reduction capability is more related to available active sites for Cr(VI) reduction rather than their surface area. Furthermore, the photoetching of the semiconductors by Cr(VI) also reduced their photocatalytic reduction ability.[33b]

4.2.2. Other Photocatalysts

Graphitic carbon nitride (g-C_3N_4) is a less toxic, metal-free organic semiconductor having a visible light response, whose band gap is 2.7 eV, which has been widely reported for the removal of various pollutants.[49] The photocatalytic activity of g-C_3N_4 can be enhanced by treating with the NaOH solution treated method.[50] Under visible light, the Cr(VI) reduction ratio was improved from 29.4% to 100% for 300 mL aqueous solution containing 50 mg/L of $K_2Cr_2O_7$. The improved reduction rate was due to the porous structure of the alkali treated g-C_3N_4 thin nanoplates which shortened the distance of transportation for photogenerated holes and electrons to the solid-liquid interface from the generated sites, that reduced their recombination.

Bi_2S_3 is a typical lamellar structured semiconductor having a direct band gap of 1.3 eV. Because of the narrow band gap and large absorption coefficient, it is one of the important visible-light responsive photocatalysts. Special morphology, such as hollow nanosphere shaped Bi_2S_3 is the research focus on the photocatalytic reduction of Cr(VI).[51] Besides, through a facile ethanol-assisted one-pot reaction, Bi_2S_3 nanostructures of different morphologies such as nanowires (NWs), nanorods (NRs), and nanotubes (NTs) have been prepared. Among them, Bi_2S_3 NWs displayed the highest photocatalytic activity towards the Cr(VI) reduction under visible light exposure. After 60 min of exposure, Bi_2S_3 nanowires reduced nearly 85.1% of Cr(VI) whereas NRs and NTs reduced about 69.9% and 66.1% of Cr(VI), respectively. Moreover, NWs can be reused after an acid wash in dilute HCl.[52]

4.2.3. Composite Photocatalysts

Generally, a composite of two individual photocatalysts exhibits higher photocatalytic efficiency than their individual constituents, because of their synergistic effect that enhances the electron-hole separation and charges transportation.[53] For example, the $k_2Ti_6O_{13}$-TiO_2 composite sample obtained by the calcination of TiO_2 impregnated by KOH,[39] exhibited higher rate constant of $3.07\times10^{-7}\,Ms^{-1}$ than that of $k_2Ti_6O_{13}$ ($1.38\times10^{-7}\,Ms^{-1}$). The enhanced photocatalytic reduction activity could be ascribed to the interaction between $K_2Ti_6O_{13}$ and the anatase TiO_2. The interaction between $K_2Ti_6O_{13}$ and the anatase TiO_2 denotes the charge transfer between the $K_2Ti_6O_{13}$ and the anatase TiO_2. Under illumination, $K_2Ti_6O_{13}$ (CB potential = −1.0 Vs NHE) injects electrons from its conduction band into the conduction band of the anatase TiO_2 (CB potential = 0.3 Vs NHE) and reduces the Cr(VI) that preferentially adsorb on the surface of anatase TiO_2. The augmentation of electrons in the conduction band of the anatase TiO_2 due to the energy transfer enhanced the performance of $K_2Ti_6O_{13}/TiO_2$.[54]

Besides, three-dimensional (3D) TiO_2-graphene hydrogel composite is prepared to reduce Cr(VI) under UV irradiation. The 3D hydrogel was obtained by heating the mixture of TiO_2, graphene oxide and polyethylene glycol at 95 °C for 1 h, followed by freeze-drying for 24 h. The TiO_2-graphene hydrogel material exhibited outstanding adsorption-photocatalysis performance. It removed 100% of Cr(VI) from a 100 mL (10 mg/L Cr(VI)) solution within 30 min under UV exposure. There into, the graphene contributed to the fast and high capacity adsorption; and the synergism between TiO_2 and graphene promoted photo-induced electron-hole separation and their transport, thereby facilitated the photocatalytic reduction of Cr(VI).[55]

4.2.4. Doped Photocatalysts

Doping of semiconductors with metal cations, such as Li^+, Zn^{2+}, Cd^{2+}, Ce^{3+}, $Mn^{2+,}$ and Fe^{3+}, significantly improved their photocatalytic activity.[56] Amongst them, Li^+ doped TiO_2 displayed the highest activity towards the decomposition of pollutants.[57] The 0.2 g Li^+ doped TiO_2 prepared by the ionic liquid-assisted hydrothermal method reduced the 1×10^{-3} mol/L Cr (VI) in 100 mL of $K_2Cr_2O_7$ solution to Cr(III) in about 75 min under UV-light exposure.[58] While the pristine TiO_2 nanoparticles reduced the same amount in 120 min. This showed that the doping of metal cations improved the reduction rate. Photocatalytic Au doped TiO_2 nanospheres (TiO_2-Au NSs, the diameter is about 206 nm) exhibited a reduction rate that was 4.3 and 1.8 fold faster than that of P25 and TiO_2 NSs, respectively towards the reduction of Cr(VI) to Cr(III). It was also more rapid relative to ZnO and $BiVO_4$ in the reduction of Cr(VI).[35a,59]

At present, metal-organic frameworks (MOFs) are an emerging direction in the field of photocatalysis. MOFs immobilized with metal nanoparticles (such as Au, Pd, Pt) have been prepared by a room-temperature photo-deposition technique to investigate their Cr(VI) reduction ability.[60] The metal nanoparticles doped MOF [M@MIL-100 (Fe)] exhibited improved photocatalytic activities toward heavy-metal Cr(VI) ions under the exposure of visible-light ($\lambda > 420$ nm) comparing with pristine MOF [MIL-100 (Fe)]. The enhanced photocatalytic activities are ascribed to the combined effect of the improved light absorption and photogenerated charge carrier separation, Figure 3.

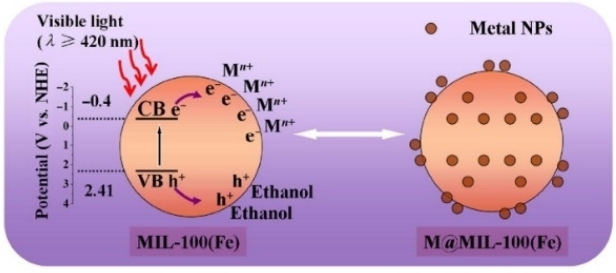

Figure 3. Formation of M@MIL-100 (Fe) nanocomposites by Photodeposition route. CB: conduction band; VB: valence band; M: Au, Pd, Pt; e^-: photoexcited electrons; h^+: photoexcited holes; NPs: nanoparticles. Reproduced with permission from ref.[60] Copyrights © Tsinghua University Press and Springer-Verlag Berlin Heidelberg 2015.

4.2.5. p–n Heterojunction Photocatalyst

p-n Heterojunction structure formed by combining the p-type and n-type semiconductors can effectively suppress the electron-hole recombination.[61] Theoretically, an inner electric field was formed at the p-n heterojunction due to the accumulation of holes and electrons at the interface of the n-type and p-type region, respectively. This inner electric field contributed to the efficient separation of the photogenerated holes and electrons as shown in Figure 4a. For example, Wei et al. demonstrated that the p-n heterojunction of n-$BiVO_4$@p-MoS_2 core-shell structure (Figure 4a) displayed an enhanced photocatalytic activity towards Cr(VI) reduction than the pristine p-type MoS_2 and n-type $BiVO_4$.[62] The enhanced reduction ratio is due to the reduced charge recombination at the p-n heterojunction structure along with their high surface area and good adsorption ability towards the Cr (VI).

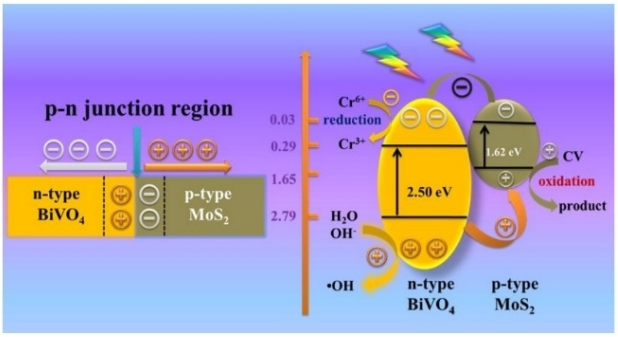

Figure 4. The formation model and the mechanism of p-n heterojunction photocatalyst. Reproduced with permission from ref.[62] Copyrights © 2015 Elsevier B.V.

4.3. Photoelectrocatalytic (PEC) Reduction of Cr(VI)

Even though the combined chromium reduction and organic pollutant oxidation enhanced the photoreduction rate as mentioned in section 4.1.3, the higher electron-hole pair recombination is a major limitation to their application. Photoelectrocatalytic oxidation has been reported as another attractive way to impede the electron/hole recombination.[63] In this system, a bias potential applied across the catalyst supported photoanode that can help to separate photo-generated electrons and holes. So photoelectrocatalysis is more efficient than photocatalysis. (as shown in the following Figure 5[16b])

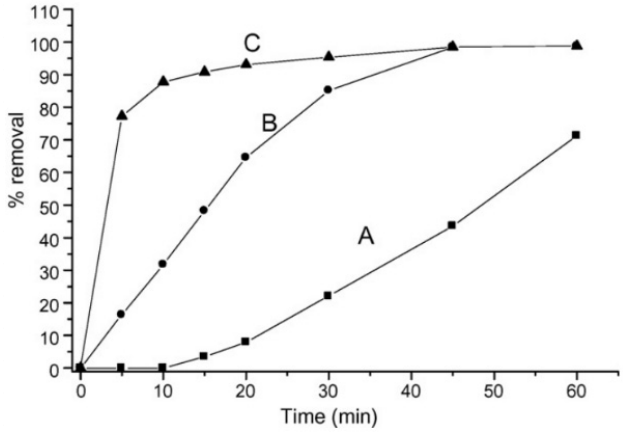

Figure 5. Removal percentage of acid dye 151: (A) photolytic; (B) photocatalytic and (C) photoelectrocatalytic treatments. Reproduced with permission from ref.[16b] Copyrights © 2008 Elsevier B.V.

Another advantage of PEC is the immobilization of photocatalysts on a fixed transparent surface other than the use of suspensions. This eliminates the expensive and time-consuming separation and recycling process of the ultrafine catalyst.[64] Despite their higher photocatalytic efficiency, only a few studies have been reported for the reduction of Cr(VI) using PEC.

Simultaneous photoelectrocatalytic oxidation of anionic surfactant and reduction of Cr(VI) were studied by Paschoal et al. At an initial concentration of Cr(VI) between 1.47 and 88.2 mg/L, about 97.7% to 100% of Cr(VI) removal was achieved through PEC. In this process, nanoporous Ti/TiO_2 was used as photoanode and platinum gauze as the auxiliary electrode. The photoelectrocatalytic oxidation promoted 100% discoloration, reduced 95% of the original total organic carbon, and 98–100% of Cr(VI). The PEC reduction rate of Cr(VI) was higher than that of the PC method.[16b]

Besides, Cr(VI) is also reduced photoelectrocatalytically in the photoelectrochemical cell comprising TNT as photoanode and Ti mesh as the photocathode. TNT offered a higher light energy trapping than that of TiO_2 thin films.[65] Further, the photoelectrocatalytic activity of TNT can be tuned by tailoring their length. Among the TNT of different lengths, TNT with shorter length displayed much greater PEC activity; because the shorter TNT efficiently transferred the electrons more effectively than that of larger TNT (Figure 6). Under the UV exposure for 60 min, 200 mL of a solution containing 17.7 mg/L Cr(VI) was completely reduced. In addition, the TNT with smaller length exhibited a longer life cycle, indicating their potential for large-scale application.[16c,66]

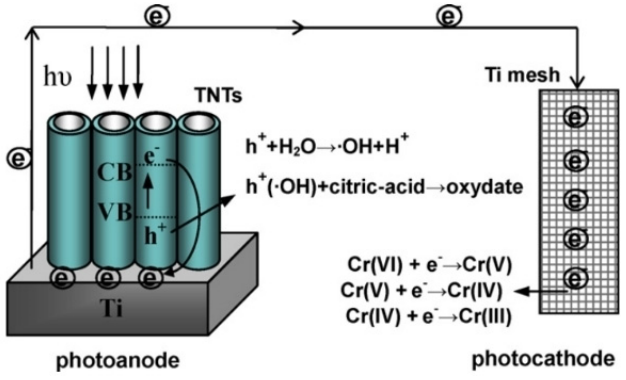

Figure 6. Mechanism of the Cr(VI) reduction of PEC with S-TNT as the photoanode and the Ti mesh as the photocathode under UV irradiation. Reproduced with permission from ref.[16c] Copyrights © 2010 Elsevier B.V.

Meanwhile, X. Feng et al. demonstrated a reduction of Cr(VI) by the photo-induced electrons generated from the citric acid using a novel PEC configuration. The PEC cell consisted of Ti photoanode, platinum photocathode and citric acid and Cr(VI) in the solution. At a bias of 1.5 V, the PEC displayed 3 times higher rate constant than the PEC cell comprising of ITO/TiO_2 photoanode and Ti photocathode.

The authors proposed that an energy-relay cascade formed by Ti photoanode, citric acid, and Cr(VI) improved the Cr(VI) reduction. This cell did not need organic dye for metal oxide photocatalysts and hence it could be potential low cost and environmentally friendly method in the wastewater treatment.[67]

As mentioned above, new adsorbent materials and new photocatalysts for the removal of chromium pollution appear continuously in recent years. At the same time, new techniques, such as the photoelectrocatalytic reduction of Cr(VI) also appear. The invention of new techniques and equipment is more important in the practice of the Cr(VI) contaminated water treatment.

7. Conclusion and Perspectives

The review discusses new adsorbent materials for the removal of chromium in contaminated wastewater. These adsorbent materials include modified diatomaceous earth and magnetic iron oxide, nano-γ-Al_2O_3, a chitosan derivative, PAN and its composites etc. Then the review focuses on the photocatalytic reduction of Cr(VI) method. The main influencing factors such as catalyst activity, solution pH, Cr adsorption on the catalyst, and additives are also briefly discussed concerning the reduction efficiency of Cr(VI). Particular highlight focuses on photoelectrocatalytic (PEC) reduction of Cr(VI). The photocatalytic and photoelectrocatalytic reduction was found to be advantageous over other conventional methods due to their easy installation, less expensive, high efficacy and low energy consumption.

Besides these advantages, there are still some challenges such as no clear understanding on many factors including surface area, particle size, surface defects and adsorption capacity that affects the Cr (VI) reduction efficiency of the photocatalysts. As a result, efforts should be taken towards developing appropriate strategies to achieve high-performance and stable photocatalyts. The photoelectrocatalytic (PEC) reduction is more efficient than photocatalytic reduction because PEC effectively separates the photo-generated electron-hole pairs. Moreover, to improve the performance PEC reduction, the following factors need to be considered: (i) electron transport kinetics from photoanode to Cr(VI) and (ii) electrons transport between the cathode and the Cr(VI) for its reduction while new photocatalysts are to be designed and prepaerd. However, photoelectrocatalytic (PEC) reduction is envisioned to be promising for high-efficiency reduction of Cr(VI).

Acknowledgements

This project is financially supported by the Fundamental Research Funds for the Central Universities of China No. 2652017150, and the innovative experiment projects of China University of Geosciences (Beijing) No. 2017BXY033, No. 2017BXY034.

References

[1] a) B. Qiu, C. Xu, D. Sun, Q. Wang, H. Gu, X. Zhang, B. L. Weeks, J. Hopper, T. C. Ho, Z. Guo, S. Wei, *Appl. Surf. Sci.* **2015**, *334*, 7–14; b) K. Gong, Q. Hu, L. Yao, M. Li, D. Sun, Q. Shao, B. Qiu, Z. Guo, *ACS Sustainable Chem. Eng.* **2018**, *6*, 7283–7291.

[2] a) S. M. Hegde, R. L. Babu, E. Vijayalakshmi, R. H. Patil, M. Naveen Kumar, K. M. Kiran Kumar, R. Nagesh, K. Kavya, S. C. Sharma, *Desalin. Water Treat.* **2016**, *57*, 8504–8513; b) K. Gong, Q. Hu, Y. Xiao, X. Cheng, H. Liu, N. Wang, B. Qiu, Z. Guo, *J. Mater. Chem. A* **2018**, *6*, 11119–11128; c) Y. Ma, L. Lv, Y. Guo, Y. Fu, Q. Shao, T. Wu, S. Guo, K. Sun, X. Guo, E. K. Wujcik, Z. Guo, *Polymer* **2017**, *128*, 12–23.

[3] a) V. K. Gupta, A. Rastogi, *J. Hazard. Mater.* **2009**, *163*, 396–402; b) C.-L. Lin, J.-X. Zhang, L. Lan, *Desalin. Water Treat.* **2015**, *54*, 637–641; c) Y.-P. Wang, P. Zhou, S.-Z. Luo, S. Guo, J. Lin, Q. Shao, X. Guo, Z. Liu, J. Shen, B. Wang, Z. Guo, *Adv. Polym. Technol.* **2018**, in press, doi: 10.1002/adv.21969.

[4] a) M. Costa, *Toxicol. Appl. Pharmacol.* **2003**, *188*, 1–5; b) R. A. Abu-Zurayk, R. Z. Al Bakain, I. Hamadneh, A. H. Al-Dujaili, *J. Mineral.* **2015**, *140*, 79–87.

[5] M. Kumari, C. U. Pittman, D. Mohan, *J. Colloid Interface Sci.* **2015**, *442*, 120–132.

[6] B. Qiu, J. Guo, X. Zhang, D. Sun, H. Gu, Q. Wang, H. Wang, X. Wang, X. Zhang, B. L. Weeks, Z. Guo, S. Wei, *ACS Appl. Mater. Interfaces* **2014**, *6*, 19816–19824.

[7] H. J. Wiegand, H. Ottenwälder, H. M. Bolt, *Toxicology* **1984**, *33*, 341–348.

[8] W. Liu, J. Ni, X. Yin, *Water Res.* **2014**, *53*, 12–25.

[9] L.-Y. Chang, *Environ. Prog.* **2004**, *22*, 174–182.

[10] a) A. Rehman, F. R. Shakoori, A. R. Shakoori, *Bioresour. Technol.* **2008**, *99*, 3890–3895; b) J. Huang, Y. Cao, Q. Shao, X. Peng, Z. Guo, *Ind. Eng. Chem. Res.* **2017**, *56*, 10689–10701.

[11] a) F. Gode, E. Pehlivan, *J. Hazard. Mater.* **2003**, *100*, 231–243; b) S. Rengaraj, C. K. Joo, Y. Kim, J. Yi, *J. Hazard. Mater.* **2003**, *102*, 257–275.

[12] a) X. N. Sun, A. P. Liu, Q. F. Chen, X. Wang, *Int. J. Mod. Phys. B* **2015**, *29*, 1542044; b) S.-S. Chen, C.-Y. Cheng, C.-W. Li, P.-H. Chai, Y.-M. Chang, *J. Hazard. Mater.* **2007**, *142*, 362–367.

[13] a) Z. Modrzejewska, W. Kaminski, *Ind. Eng. Chem. Res.* **1999**, *38*, 4946–4950; b) Q. Hu, D. Sun, Y. Ma, B. Qiu, Z. Guo, *Polymer* **2017**, *120*, 236–243; c) C. Lin, B. Fan, J. X. Zhang, X. Yang, H. Zhang, *Desalin. Water Treat.* **2016**, *57*, 21627–21633; d) X. Jiang, S. Li, S. He, Y. Bai, L. Shao, *J. Mater. Chem. A* **2018**, *6*, 15064–15073; e) J. Gu, Y. Li, C. Liang, Y. Tang, L. Tang, Y. Zhang, J. Kong, H. Liu, Z. Guo, *J. Mater. Chem. C* **2018**, *6*, 7652–7660; f) H. Sun, X. Yang, Y. Zhang, X. Cheng, Y. Xu, Y. Bai, L. Shao, *J. Membr. Sci.* **2018**, *563*,

22–30; g) X. Yang, Z. Wang, L. Shao, *J. Membr. Sci.* **2018**, *549*, 67–74.
[14] a) A. Shokati Poursani, A. Nilchi, A. H. Hassani, M. Shariat, J. Nouri, *Int. Environ. Saf.* **2015**, *12*, 2003–2014; b) V. K. Gupta, M. Gupta, S. Sharma, *Water Res.* **2001**, *35*, 1125–1134; c) M. Rao, A. V. Parwate, A. G. Bhole, *Waste Manage.* **2002**, *22*, 821–830; d) J. Huang, Y. Li, Y. Cao, F. Peng, Y. Cao, Q. Shao, H. Liu, Z. Guo, *J. Mater. Chem. A* **2018**, *6*, 13062–13074; e) Z. Xiang, R. Mercado, J. M. Huck, H. Wang, Z. Guo, W. Wang, D. Cao, M. Haranczyk, B. Smit, *J. Am. Chem. Soc.* **2015**, *137*, 13301–13307.
[15] a) A. Schmieman Eric, R. Yonge David, A. Rege Mahesh, N. Petersen James, E. Turick Charles, L. Johnstone Donald, A. Apel William, *J. Environ. Eng.* **1998**, *124*, 449–455; b) E. Fosso-Kankeu, H. Mittal, F. Waanders, I. O. Ntwampe, S. S. Ray, *Int. Environ. Saf.* **2016**, *13*, 711–724; c) M. Ziagova, G. Dimitriadis, D. Aslanidou, X. Papaioannou, E. Litopoulou Tzannetaki, M. Liakopoulou-Kyriakides, *Bioresour. Technol.* **2007**, *98*, 2859–2865.
[16] a) Z. Zhao, B. Zhang, D. Chen, Z. Guo, Z. Peng, *J. Nanosci. Nanotechnol.* **2016**, *16*, 2847–2852; b) F. M. M. Paschoal, M. A. Anderson, M. V. B. Zanoni, *J. Hazard. Mater.* **2009**, *166*, 531–537; c) Q. Wang, J. Shang, T. Zhu, F. Zhao, *J. Mol. Catal. A* **2011**, *335*, 242–247.
[17] a) Q. Yan, Z. Zhang, Y. Zhang, A. Umar, Z. Guo, D. O'Hare, Q. Wang, *Eur. J. Inorg. Chem.* **2015**, *2015*, 4182–4191; b) L. Chen, H. Wang, H. Wei, Z. Guo, M. A. Khan, D. P. Young, J. Zhu, *RSC Adv.* **2015**, *5*, 42540–42547; c) Z. Xiang, Z. Hu, D. Cao, W. Yang, J. Lu, B. Han, W. Wang, *Angew. Chem. Int. Ed.* **2010**, *50*, 491–494; d) Y. Song, L. He, X. Zhang, F. Liu, N. Tian, Y. Tang, J. Kong, *J. Phys. Chem. C* **2017**, *121*, 24774–24785.
[18] a) F. T. R. d. Almeida, B. C. S. Ferreira, A. L. d. S. L. Moreira, R. P. d. Freitas, L. F. Gil, L. V. A. Gurgel, *J. Colloid Interface Sci.* **2016**, *466*, 297–309; b) Y.-P. Wang, P. Zhou, S.-Z. Luo, S. Guo, J. Lin, Q. Shao, X. Guo, Z. Liu, J. Shen, B. Wang, Z. Guo, *Adv. Polym. Technol.* **2018**, *0*, 1–16.
[19] I. H. Kim, J.-H. Choi, J. O. Joo, Y.-K. Kim, J.-W. Choi, B.-K. Oh, *J. Microb. Biotechnol.* **2015**, *25*, 1542–1546.
[20] Y. Du, L. Wang, J. Wang, G. Zheng, J. Wu, H. Dai, *J. Environ. Sci.* **2015**, *29*, 71–81.
[21] R. Z. Al Bakain, R. A. Abu-Zurayk, I. Hamadneh, F. I. Khalili, A. H. Al-Dujaili, *Desalin. Water Treat.* **2015**, *56*, 826–838.
[22] a) N. Waijarean, K. J. D. MacKenzie, S. Asavapisit, R. Piyaphanuwat, G. N. L. Jameson, *J. Mater. Sci.* **2017**, *52*, 7345–7359; b) M. Agheli, A. Habibolahzadeh, *Protection of Metals Phys. Chem. Surfaces* **2016**, *52*, 972–974; c) A. Shokati Poursani, A. Nilchi, A. Hassani, S. Tabibian, L. Asad Amraji, *Int. J. Environ. Technol. Manage.* **2017**, *14*, 1459–1468; d) Y.-P. Wang, P. Zhou, S.-Z. Luo, X.-P. Liao, B. Wang, Q. Shao, X. Guo, Z. Guo, *Langmuir* **2018**, *34*, 7859–7868.
[23] F. Gao, H. Gu, H. Wang, X. Wang, B. Xiang, Z. Guo, *RSC Adv.* **2015**, *5*, 60208–60219.
[24] a) G. Ren, X. Wang, P. Huang, B. Zhong, Z. Zhang, L. Yang, X. Yang, *Sci. Total Environ.* **2017**, *607–608*, 900–910; b) R. Khani, S. Sobhani, M. H. Beyki, *J. Colloid Interface Sci.* **2016**, *466*, 198–205; c) Z. Liu, L. Chen, L. Zhang, S. Poyraz, Z. Guo, X. Zhang, J. Zhu, *Chem. Commun.* **2014**, *50*, 8036–8039; d) L. Yang, D. Cheng, H. Xu, X. Zeng, X. Wan, J. Shui, Z. Xiang, D. Cao, *Proc. Natl. Acad. Sci. USA* **2018**, *115*, 6626; e) L. Yang, L. Shi, D. Wang, Y. Lv, D. Cao, *Nano Energy* **2018**, *50*, 691–698.
[25] J.-l. Lv, Q.-d. An, W. Zheng, Y. Fan, Z.-m. Lei, S.-r. Zhai, *J. Inst. Chem.* **2016**, *65*, 312–322.
[26] C. Luo, W. Duan, X. Yin, J. Kong, *J. Phys. Chem. C* **2016**, *120*, 18721–18732.
[27] C. Zhang, X. Li, X. Bian, T. Zheng, C. Wang, *J. Hazard. Mater.* **2012**, *229–230*, 439–445.
[28] A. Mohamed, W. S. Nasser, T. A. Osman, M. S. Toprak, M. Muhammed, A. Uheida, *J. Colloid Interface Sci.* **2017**, *505*, 682–691.
[29] S. Haider, S.-Y. Park, *J. Membr. Sci.* **2009**, *328*, 90–96.
[30] S. Zhou, F. Liu, Q. Zhang, B.-Y. Chen, C.-J. Lin, C.-T. Chang, *J. Nanosci. Nanotechnol.* **2015**, *15*, 5823–5832.
[31] a) W. S. Wan Ngah, L. C. Teong, M. A. K. M. Hanafiah, *Carbohydr. Polym.* **2011**, *83*, 1446–1456; b) T. Wu, Q. Shao, S. Ge, L. Bao, Q. Liu, *RSC Adv.* **2016**, *6*, 58020–58027.
[32] a) S. M. Lee, Lalchhingpuii, Lalhmunsiama, D. Tiwari, *Chem. Eng. J.* **2016**, *296*, 35–44; b) F. G. L. Medeiros Borsagli, A. A. P. Mansur, P. Chagas, L. C. A. Oliveira, H. S. Mansur, *React. Funct. Polym.* **2015**, *97*, 37–47; c) T. Wu, Q. Shao, S. Ge, W. Zhao, Q. Liu, *Mater. Res. Bull.* **2016**, *83*, 657–663.
[33] a) W. Yao, P. Rao, I. M. C. Lo, W. Zhang, W. Zheng, *J. Environ. Sci.* **2014**, *26*, 2379–2386; b) R. Karthik, S. Meenakshi, *Int. J. Biol. Macromol.* **2014**, *67*, 210–219; c) H. Gu, X. Xu, H. Zhang, C. Liang, H. Lou, C. Ma, Y. Li, Z. Guo, J. Gu, *Eng. Sci.* **2018**, *1*, 46–54; d) Z. Zhao, R. Guan, J. Zhang, Z. Zhao, P. Bai, *Acta Metall. Sin. (Engl. Lett.)* **2017**, *30*, 66–72; e) Z. Zhao, P. Bail, R. Guan, V. Murugadoss, H. Liu, X. Wang, Z. Guo, *Mater. Sci. Eng. A* **2018**, *734*, 200–209; f) Y. Zhao, L Qi, Y Jin, K. Wang, J. Tian, P. Han, *J. Alloys Compd.* **2015**, *647*, 1104–1110; g) Y. Zhao, S. Deng, H. Liu, J. Zhang, Z. Guo, H. Hou, *Comput. Mater. Sci.* **2018**, *154*, 365–370.
[34] a) H. Gu, S. B. Rapole, J. Sharma, Y. Huang, D. Cao, H. A. Colorado, Z. Luo, N. Haldolaarachchige, D. P. Young, B. Walters, S. Wei, Z. Guo, *RSC Adv.* **2012**, *2*, 11007–11018; b) K. Gong, S. Guo, Y. Zhao, Q. Hu, H. Liu, D. Sun, M. Li, B. Qiu, Z. Guo, *J. Mater. Chem. A* **2018**, *6*, 16824–16832.
[35] a) L. B. Khalil, W. E. Mourad, M. W. Rophael, *Appl. Catal. B* **1998**, *17*, 267–273; b) H. Yoneyama, Y. Yamashita, H. Tamura, *Nature* **1979**, *282*, 817; c) J. Doménech, J. Muñoz, *Electrochim. Acta* **1987**, *32*, 1383–1386.
[36] D. Chen, A. K. Ray, *Chem. Eng. Sci.* **2001**, *56*, 1561–1570.
[37] a) S. Wang, Z. Wang, Q. Zhuang, *Appl. Catal. B* **1992**, *1*, 257–270; b) L. Zhang, M. Qin, W. Yu, Q. Zhang, H. Xie, Z. Sun, Q. Shao, X. Guo, L. Hao, Y. Zheng, Z. Guo, *J. Electrochem. Soc.* **2017**, *164*, H1086-H1090.
[38] S.-S. Ge, Q.-X. Zhang, X.-T. Wang, H. Li, L. Zhang, Q.-Y. Wei, *Surf. Coat. Technol.* **2015**, *283*, 172–176.
[39] S. Zheng, Z. Xu, Y. Wang, Z. Wei, B. Wang, *J. Photochem. Photobiol. A* **2000**, *137*, 185–189.

[40] D. Pan, S. Ge, X. Zhang, X. Mai, S. Li, Z. Guo, *Dalton Trans.* **2018**, *47*, 708–715.
[41] M. D. Ward, J. R. White, A. J. Bard, *J. Am. Chem. Soc.* **1983**, *105*, 27–31.
[42] Y. Ku, I.-L. Jung, *Water Res.* **2001**, *35*, 135–142.
[43] J.-M. Herrmann, H. Tahiri, C. Guillard, P. Pichat, *Catal. Today* **1999**, *54*, 131–141.
[44] G. Colón, M. C. Hidalgo, J. A. Navío, *Langmuir* **2001**, *17*, 7174–7177.
[45] E. Pelizzetti, C. Minero, *Electrochim. Acta* **1993**, *38*, 47–55.
[46] H. Fu, G. Lu, S. Li, *J. Photochem. Photobiol. A* **1998**, *114*, 81–88.
[47] R. Chaudhary, R. S. Thakur, *Renewable Sustainable Energy Rev.* **2012**, *4*, 053121.
[48] a) R. S. Thakur, R. Chaudhary, C. Singh, *Desalin. Water Treat.* **2015**, *56*, 1335–1363; b) J.-x. Zhang, S. Liu, C. Yan, X.-j. Wang, L. Wang, Y.-m. Yu, S.-y. Li, *Nanoscience* **2017**, *7*, 691–700; c) J. Zhao, S. Ge, D. Pan, Q. Shao, J. Lin, Z. Wang, Z. Hu, T. Wu, Z. Guo, *J. Colloid Interface Sci.* **2018**, *529*, 111–121; d) L. Yang, X. Wang, X. Mai, T. Wang, C. Wang, X. Li, V. Murugadoss, Q. Shao, S. Angaiah, Z. Guo, *J. Colloid Interface Sci.* **2019**, *534*, 459–468.
[49] X. Wang, Y. Liang, W. An, J. Hu, Y. Zhu, W. Cui, *Appl. Catal. B* **2017**, *219*, 53–62.
[50] Q. Zhang, S. Liu, Y. Zhang, A. Zhu, J. Li, X. Du, *Mater. Lett.* **2016**, *171*, 79–82.
[51] S. Luo, F. Qin, Y. a. Ming, H. Zhao, Y. Liu, R. Chen, *J. Hazard. Mater.* **2017**, *340*, 253–262.
[52] E. Hu, X. Gao, A. Etogo, Y. Xie, Y. Zhong, Y. Hu, *J. Alloys Compd.* **2014**, *611*, 335–340.
[53] a) J. Lei, Q. Shao, X. Wang, Q. Wei, L. Yang, H. Li, Y. Huang, B. Hou, *Mater. Res. Bull.* **2017**, *95*, 253–260; b) S. Ge, Q. Zhang, X. Wang, Q. Shao, L. Bao, R. Ding, Q. Liu, *J. Nanosci. Nanotechnol.* **2016**, *16*, 4929–4935; c) L. Zhang, W. Yu, C. Han, J. Guo, Q. Zhang, H. Xie, Q. Shao, Z. Sun, Z. Guo, *J. Electrochem. Soc.* **2017**, *164*, H651-H656.
[54] S. Uchida, Y. Yamamoto, Y. Fujishiro, A. Watanabe, O. Ito, T. Sato, *J. Chem. Soc. Faraday Trans.* **1997**, *93*, 3229–3234.
[55] Y. Li, W. Cui, L. Liu, R. Zong, W. Yao, Y. Liang, Y. Zhu, *Appl. Catal. B* **2016**, *199*, 412–423.
[56] H. L. Shindume, Z. Zhao, W. Ning, L. Hu, A. Umar, J. Zhang, T. Wu, Z. Guo, *J. Nanosci. Nanotechnol.* **2019**, *19*, 839–849.
[57] a) Y. Bessekhouad, D. Robert, J. V. Weber, N. Chaoui, *J. Photochem. Photobiol. A* **2004**, *167*, 49–57; b) M. Zamora, T. López, R. Gómez, M. Asomoza, A. GarcÍa-Ruiz, X. Bokhimi, *J. Sol-Gel Sci. Technol.* **2004**, *32*, 339–343.
[58] T. N. Ravishankar, G. Nagaraju, J. Dupont, *Mater. Res. Bull.* **2016**, *78*, 103–111.
[59] a) R. Ravindranath, P. Roy, A. P. Periasamy, H.-T. Chang, *RSC Adv.* **2014**, *4*, 57290–57296; b) B. Xie, H. Zhang, P. Cai, R. Qiu, Y. Xiong, *Chemosphere* **2006**, *63*, 956–963.
[60] R. Liang, F. Jing, L. Shen, N. Qin, L. Wu, *Nano Res.* **2015**, *8*, 3237–3249.
[61] C. Han, Q. Shao, J. Lei, Y. Zhu, S. Ge, *J. Alloys Compd.* **2017**, *703*, 530–537.
[62] W. Zhao, Y. Liu, Z. Wei, S. Yang, H. He, C. Sun, *Appl. Catal. B,* **2016**, *185*, 242–252.
[63] P. A. Carneiro, M. E. Osugi, J. J. Sene, M. A. Anderson, M. V. B. Zanoni, *Electrochim. Acta* **2004**, *49*, 3807–3820.
[64] a) A. K. Ray, A. A. C. M. Beenackers, *Catal. Today* **1998**, *40*, 73–83; b) K. Ray Ajay, A. C. M. Beenackers Antonie, *AIChE J.,* **2004**, *44*, 477–483; c) S. Mukherjee Preety, K. Ray Ajay, *Chem. Eng. Technol.* **1999**, *22*, 253–260.
[65] C. Han, Q. Shao, M. Liu, S. Ge, Q. Liu, J. Lei, *Mater. Sci. Semicond. Process.* **2016**, *56*, 166–173.
[66] H. Song, J. Shang, J. Ye, Q. Li, *Thin Solid Films* **2014**, *551*, 158–162.
[67] X. Feng, J. Shang, T. Zhu, *Electrochim. Acta* **2016**, *188*, 752–756.

Received: September 7, 2018
Accepted: October 19, 2018
Published online on November 14, 2018

